Available online at www.sciencedirect.com
ScienceDirect
European Journal of Medicinal Chemistry 42 (2007) 544–551
EUROPEAN JOURNAL OF MEDICINAL CHEMISTRY
http://www.elsevier.com/locate/ejmech

Short communication

Syntheses, characterization and in vitro antiamoebic activity of new Pd(II) complexes with 1-*N*-substituted thiocarbamoyl-3,5-diphenyl-2-pyrazoline derivatives

Asha Budakoti, Mohammad Abid, Amir Azam*

Department of Chemistry, Jamia Millia Islamia, Jamia Nagar, New Delhi 110025, India

Received 22 December 2005; received in revised form 3 October 2006; accepted 26 October 2006
Available online 6 December 2006

Abstract

Reaction of neutral NS bidentate ligands, 1-*N*-substituted thiocarbamoyl-3,5-diphenyl-2-pyrazolines, isolated by cyclization of chalcone with *N*-4-substituted thiosemicarbazide of aromatic amines (**1**–**8**), with $[Pd(DMSO)_2Cl_2]$ (DMSO = dimethylsulfoxide) leads to the formation of new complexes of the type $[Pd(L)Cl_2]$ (**1a**–**8a**). The structures of the compounds were elucidated by UV, IR, ^{1}H NMR, ^{13}C NMR and ESI-MS spectral data and thermogravimetric analysis and their purities were confirmed by elemental analyses. The antiamoebic activity of these complexes was evaluated by microdilution method against *HM1:IMSS* strain of *Entameoba histolytica* and the results were compared with the standard drug, metronidazole. Generally palladium complexes showed better activity than their corresponding ligands. Compound **3a** showed better $IC_{50} = 0.05$ μM as compared to metronidazole $IC_{50} = 1.82$ μM.

Keywords: Chalcone; Pyrazolines; Thiocarbamoyl; Palladium(II) complexes; Antiamoebic activity

1. Introduction

Morbidity and mortality due to enteric protozoan infection remains an important health problem worldwide mainly in developing countries and regions such as the Indian subcontinent, parts of South America and tropical part of Africa [1]. Invasive amoebiasis caused by *Entameoba histolytica* is one of the world's most prevalent and fatal infectious diseases. Patients usually suffer from diarrhea or dysentery together with a wide range of symptoms such as stomachache, cramps, bloating or tenderness [2]. Amoebic abscess of the brain is a dreadful complication of *E. histolytica* infection [3]. Pleuropulmonary amoebiasis occurs in 2–3% of patients with invasive amoebiasis and is frequently associated with liver abscess. Lung disease without liver involvement is exceptional, and it is believed that infection of the lung is a result of haematogenous spread from a primary site usually the colon [4]. Metronidazole and other nitroimidazole derivatives have been extensively used to treat infection caused by protozoa and anaerobic bacteria. However, resistance to drug as well as risk of potential mutagenicity and carcinogenicity has been described. High doses often cause side effects such as headache, dry mouth, metallic taste, glossitis and urticaria [5,6]. For these reasons, current drug therapy for amoebiasis is inadequate and efforts to identify new, selective therapeutic agents for the treatment of ameobiasis are important. Substituted pyrazolines and their derivatives have significant importance due to anti-bacterial, anti-fungal, and anti-inflammatory activities [7,8]. The pyrazole based chelating ligands form a variety of coordination complexes with a number of metal ions, providing varying coordination geometry, nuclearity and versatile properties [9–13].

Recently, we have reported the cyclized pyrazoline analogues of thiosemicarbazones and their palladium complexes [14]. It was observed that the complex, palladium{(1-*N*-adamantylamine) thiocarbamoyl-3,5-diphenyl-2-pyrazoline}chloride displayed good

* Corresponding author. Tel.: +91 11 26981717/3253; fax: +91 11 2698 0229/1232.
E-mail address: amir_sumbul@yahoo.co.in (A. Azam).

0223-5234/$ - see front matter © 2006 Published by Elsevier Masson SAS.
doi:10.1016/j.ejmech.2006.10.011

activity in vitro against *E. histolytica*. The present paper deals with the syntheses of new 1-*N*-substituted thiocarbamoyl-3,5-diphenyl-2-pyrazoline derivatives having NS donor set (**1–8**) and their palladium(II) complexes (**1a–8a**). The activity of these compounds was screened in vitro against *E. histolytica* (Table 1). Efforts to identify new, selective therapeutic agents for the treatment of ameobiasis are important due to recurrence of amoebic liver abscess even after treatment with metronidazole has been reported [15].

Table 1
In vitro antiamoebic activities of 1-*N*-substituted thiocarbamoyl-3,5-diphenyl pyrazoline derivatives and their Pd(II) complexes against (*HM1*:*IMSS*) strain of *E. histolytica*

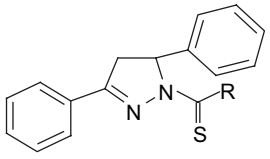

1-8

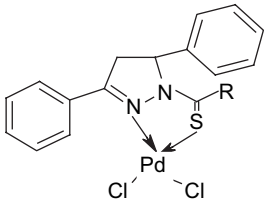

1a-8a

Compound	R	IC_{50} (μM)	SD
1	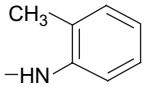	4.79	0.28
1a		4.58	0.08
2	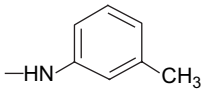	10.7	0.08
2a		1.82	0.04
3	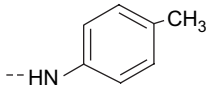	0.38	0.03
3a		0.05	0.04
4	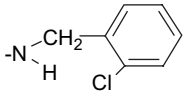	11.0	0.05
4a		1.24	0.07
5	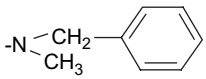	2.80	0.02
5a		0.70	0.05
6	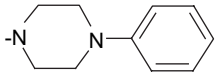	1.8	0.20
6a		0.76	1.04
7	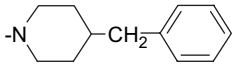	1.60	0.05
7a		0.40	0.02
8	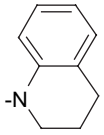	0.45	0.03
8a		1.10	0.08
	$[Pd(DMSO)_2Cl_2]$	8.15	1.73
	Metronidazole	1.82	0.1

SD = standard deviation.

2. Results and discussion

Under the reaction condition, reaction mixture contained only unreacted starting material and the cyclized product in poor yield. The yield of cyclized product in substituted thiosemicarbazide was in the range of 10–30%. The precursor used for the synthesis of Pd(II) complexe $[Pd(DMSO)_2Cl_2]$ was synthesized by the literature procedure [16]. All the Pd(II) complexes were prepared by mixing an equimolar ratio of ligand and $[Pd(DMSO)_2Cl_2]$ in refluxing methanol and gave 65–87% yield (Scheme 1). The obtained compounds are stable in the solid as well as in the solution state (Table 2).

2.1. IR and electronic spectral studies

The IR data were very informative and provided evidence for the formation of the expected structures. In the IR of starting material chalcone (C=O), (CH=CH), (C=C) function absorbed in the expected regions; (C=O) at 1664 cm^{-1}, (CH=CH) at 1620 cm^{-1} and (C=C) at 1580 cm^{-1}, respectively. The IR spectra of thiosemicarbazides were also observed in different expected regions. A sharp band due to $\nu(NH_2)$ at 3290–3355 cm^{-1} with a shoulder band at 3218–3250 cm^{-1} which is absent in the IR spectra of pyrazolines and ν(C=S) at 1050–1238 cm^{-1}. All the compounds (**1–8**) showed intense bands in the region 1333–1370 cm^{-1} due to the ν(C=S) stretching of the thiocarbamoyl group. The IR spectra of all the compounds showed ν(C=N) stretching at 1542–1590 cm^{-1} due to the ring closure. In addition, the absorption bands at 1024–1122 cm^{-1} were attributed to the ν(C–N) stretching vibrations, which also confirm the formation of desired pyrazoline ring in all the compounds. The compounds (**1–4**) showed additional sharp bands in the region 3421–3448 cm^{-1} due to the ν(NH) stretching. The ν(C=N) band of ligands are shifted by ca. 4–36 cm^{-1} after complexation. It indicates the involvement of azomethine nitrogen in complexation. The band due to C=S group of ligand is shifted by 5–42 cm^{-1} thereby indicating the involvement of the thione sulfur in complex formation. This contention is further confirmed by the presence of ν(Pd–N) and ν(Pd–S) band at 522–559 and 440–478 cm^{-1} in the far IR frequency region of the complexes [17].

The electronic spectral data of the ligand and their complexes are summarized in Table 3. The spectra of the ligand exhibited three absorption bands at 371–290, 288–236 and 232–205 nm assignable to $n \rightarrow \pi^*$, $\pi \rightarrow \pi^*$ and $n \rightarrow \sigma^*$ transitions, respectively. The band at 371–290 nm was assigned to the transition involving the thione portion (C=S) of thiocarbamoyl group. The two other absorption bands at 288–236 and 232–205 nm were due to $\pi \rightarrow \pi^*$ transition of phenyl ring and $n \rightarrow \sigma^*$ transition of azomethine nitrogen, respectively. In the metal complexes the bands are separated well and appeared at 366–294, 301–256, 236–205 nm due to ligand residue. In addition all the metal complexes exhibited one band in the region of 400–682 nm due to combination of sulfur–Pd(II), nitrogen–Pd(II) charge transfer (L–M) and

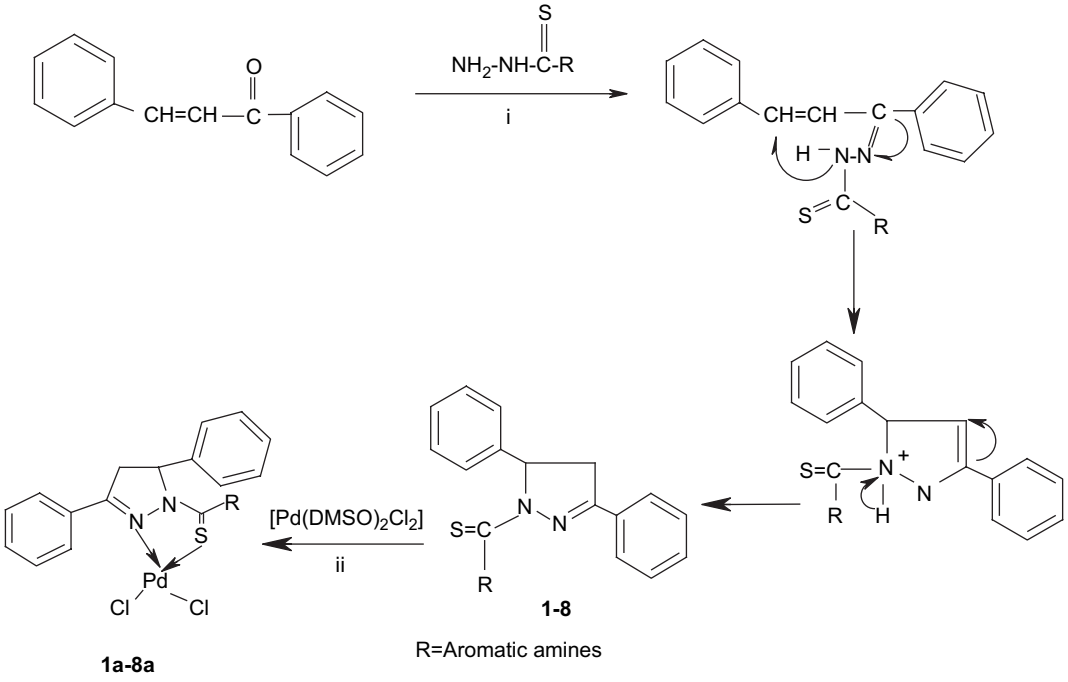

Scheme 1. Reagents and conditions (i) NaOH, ethanol, reflux (ii) dry, methanol, reflux.

Pd(II) d-d bands [18]. These observations suggest the involvement of ligands in coordination to metal ion.

2.2. Nuclear magnetic resonance spectral studies

Further evidence for the formation of pyrazoline compounds and their metal complexes were obtained from the ^{1}H NMR and ^{13}C NMR spectra (Tables 4 and 5), which provide diagnostic tools for the positional elucidation of the protons. Assignments of the signals are based on the chemical shifts and intensity patterns. The pyrazoline protons H_A and H_B (Fig. 1) are geminal protons at C_4 carbon, appears in the region of 3.64–3.31 and 3.89–3.49 ppm as doublet of doublets in all compounds. The CH proton also appears as doublet of doublets in the region of 6.32–5.91 ppm due to vicinal coupling with two nonequivalent geminal protons of C_4 carbon. The J values of the protons are (J_{AB}: 18.75–10.96, J_{AX}: 12.5–2.59, J_{BX}: 10.2–8.1 Hz) [19]. The NH proton of different substituted thiocarbamoyl compounds (**1**–**4**) showed a doublet at 10.4–7.7 ppm. In metal complexes the values of NH protons shifted upfield as compared to ligand at 9.24–7.5 ppm. The protons belonging to the aromatic ring were observed within the expected chemical shift region along with the integral values.

^{13}C NMR spectra of all the compounds were taken in $CDCl_3$ and the signal obtained further confirmed the proposed structures. The C_4 and C_5 carbons of the pyrazoline

Table 2
Elemental analysis

S. no.	Mol. formula	M.p. (°C)/dec. pt.	%Yield	C obs (calc.)	H obs (calc.)	N obs (calc)	Cl obs (calc.)	%Pd obs (calc.)
1	$C_{23}H_{21}N_3S$	175	24	74.56 (74.39)	5.61 (5.66)	11.22 (11.32)	–	–
1a	$[Pd(C_{23}H_{21}N_3S)Cl_2]$	217	72	50.63 (50.36)	3.45 (3.83)	7.89 (7.66)	12.91 (12.96)	19.11 (19.34)
2	$C_{23}H_{21}N_3S$	210	18	74.15 (74.39)	5.61 (5.66)	11.02 (11.32)	–	–
2a	$[Pd(C_{23}H_{21}N_3S)Cl_2]$	256	84	50.56 (50.36)	3.70 (3.83)	7.70 (7.66)	12.88 (12.96)	19.67 (19.34)
3	$C_{23}H_{21}N_3S$	190	13	74.80 (74.39)	5.84 (5.66)	11.57 (11.32)	–	–
3a	$[Pd(C_{23}H_{21}N_3S)Cl_2]$	250	79	50.32 (50.36)	3.31 (3.83)	7.42 (7.66)	12.43 (12.96)	19.46 (19.34)
4	$C_{23}H_{20}N_3SC1$	160	11	68.12 (68.06)	4.77 (4.96)	10.57 (10.35)	–	–
4a	$[Pd(C_{23}H_{20}N_3S)Cl_3]$	228	63	47.56 (47.38)	3.20 (3.43)	7.33 (7.21)	18.91 (18.28)	18.29 (18.21)
5	$C_{24}H_{23}N_3S$	189	22	74.68 (74.80)	5.62 (5.97)	10.62 (10.90)	–	–
5a	$[Pd(C_{24}H_{23}N_3S)Cl_2]$	241	67	51.32 (51.24)	4.62 (4.09)	7.79 (7.47)	12.83 (12.6)	18.46 (18.86)
6	$C_{26}H_{26}N_4S$	175	24	73.62 (73.23)	6.06 (6.34)	13.46 (13.14)	–	–
6a	$[Pd(C_{26}H_{26}N_4S)Cl_2]$	288	82	51.71 (51.74)	4.42 (4.31)	9.37 (9.28)	11.81 (11.77)	17.30 (17.6)
7	$C_{28}H_{28}N_3S$	182	20	76.64) (76.71)	6.66 (6.39)	9.80 (9.58)	–	–
7a	$[Pd(C_{28}H_{28}N_3S)Cl_2]$	222	79	54.64 (54.63)	4.31 (4.55)	6.88 (6.83)	11.76 (11.54)	17.15 (17.20)
8	$C_{25}H_{23}N_3S$	185	21	75.40 (75.57)	5.66 (5.79)	10.98 (10.57)	–	–
8a	$[Pd(C_{25}H_{23}N_3S)Cl_2$	220	52	52.64 (52.26)	4.31 (4.00)	7.44 (7.31)	12.19 (12.36)	18.41 (18.40)

Table 3
IR ν_{max} (cm^{-1}) and electronic spectroscopic data

Compound	ν(NH)	ν(C–H) (aromatic)	ν(C=N)	ν(C=S)	ν(C–N)	ν(Pd–N)	ν(Pd–S)	UV–vis: λ_{max} (nm)
1	3435	2924	1558	1357	1122			371, 290, 236, 217
1a	3432	2928	1536	1370	1135	452	529	707, 371, 290, 336, 217
2	3421	2922	1549	1370	1076			371, 291, 245, 223, 211
2a	3435	2924	1570	1357	1122	469	524	856, 431, 371, 290, 236, 217
3	3421	2925	1585	1350	1052			377, 270, 236, 371
3a	3438	2980	1585	1367	1150	458	524	877, 422, 371, 294, 232, 214
4	3448	2963	1542	1364	1024			371, 291, 245
4a	3435	2924	1558	1359	1124	441	522	743, 371, 290, 236, 217
5	–	2923	1545	1349	1033			366, 301, 223, 205, 246
5a	–	2926	1542	1375	1076	441	522	400, 366, 301, 246, 223, 205
6	–	2925	1578	1333	1066			371, 291, 245
6a	–	2924	1582	1364	1134	431	559	702, 401, 290, 256, 236
7	–	2928	1590	1336	1052			371, 270, 236
7a	–	2926	1542	1375	1076	440	536	682, 469, 366, 301, 223
8	–	2958	1578	1346	1082			371, 270, 236, 217
8a	–	2962	1554	1369	1088	473	536	672, 455, 366, 311, 213

ring resonate at 40.32–53.76 and 59.14–62.21 ppm, respectively. All the compounds showed a signal at 125.03–134.95 ppm, which was assigned to azomethine carbon of pyrazoline ring. Thiocarbamoyl carbon (C=S) displayed a signal at 204.23–169.42 ppm in all the compounds. The signals in the range 144.1–126.6 ppm were assumed to be due to the aromatic carbons. The azomethine carbon in the case of metal complexes showed signal in the range of 166.6–133.9 ppm and thiocarbamoyl carbon displayed a signal at 204.2–154.2 ppm due to coordination.

2.3. ESI-MS

The characteristic peaks were observed in the mass spectra of ligand and their metal complexes (Table 6), which followed the similar fragmentation pattern as reported earlier [14] (Schemes 2 and 3). The spectra of these compounds suggest that they exhibit thione–thiol tautomerisation. The fragmentation of ligand **4** showed molecular ion peak (M + 1) at 404 and occurs via cleavage of [–SH] moiety giving desired peaks at *m/z* 370. This is followed by elimination of CH_2–CN radical

Table 4
^{1}H NMR [**1**–**8**, ($CDCl_3$)], [**1a**–**8a**, ($(CD_3)_2SO$)] (δ, ppm) spectroscopic data

Compound	Aromatic	H_A	H_B	H_X	CH_3 or CH_2	N–H
1	6.72–7.50 (14H, m, Ar)	3.48 (dd, 1H, H_A, J_{AB}: 18.5, J_{AX}: 9.25)	3.49 (dd, 1H, H_B, J_{AB}: 18.5, J_{BX} 9.25)	6.32 (dd, 1H, H_X, J_{AX}: 11.10, J_{BX}: 9.25)	2.13 (s, 3H, CH_3)	9.24 (d, 1H, NH)
1a	6.72–7.55 (14H, m, Ar)	3.08 (dd, 1H, H_A)	3.69 (dd, 1H, H_B)	6.30 (dd, 1H, H_X)	2.13 (s, 3H, CH_3)	
2	6.78–7.51 (m, 14H, Ar)	3.59 (dd, 1H, H_A, J_{AB}: 18.75, J_{AX}: 12.5)	3.98 (dd, 1H, H_B, J_{AB}: 17.5, J_{BX}: 6.77)	6.32 (dd, 1H, H_X, J_{AX}: 10.96, J_{BX}: 6.77)	2.34 (s, 3H, CH_3)	6.32 (d, 1H, NH)
2a	6.72–7.50 (14H, m, Ar)	3.64 (dd, 1H, H_A)	3.89 (dd, 1H, H_B)	6.32 (dd, 1H, H_X)	2.13 (s, 3H, CH_3)	
3	6.78–7.51 (m, 10H, Ar)	3.38 (dd, 1H, H_A, J_{AB}: 17.33, J_{AX}: 9.33)	3.48 (dd, 1H, H_B, J_{AB}: 16.7, J_{BX}: 8.1)	6.21 (dd, 1H, H_X, J_{AX}: 11.6, J_{BX}: 10.2)	2.10 (s, 3H, CH_2)	9.37 (s, 1H, NH)
3a	6.72–7.50 (14H, m, Ar)	3.48 (dd, 1H, H_A)	3.49 (dd, 1H, H_B)	5.32 (dd, 1H, H_X)	2.13 (s, 3H, CH_3)	
4	6.7–7.6 (m, 14H, Ar)	3.0–2.9 (dd, 1H, H_A, J_{AB}: 18.5, J_{AX}: 9.25)	3.6 (dd, 1H, H_B, J_{AB}: 18.5, J_{BX}: 9.5)	5.9 (dd, 1H, H_X, J_{AX}: 9.25, J_{BX}: 9.5)	4.6 (d, 2H, CH_2)	9.24 (s, 1H, NH)
4a	6.72, 7.50 (14H, m, Ar)	3.59 (dd, 1H, H_A)	3.69 (dd, 1H, H_B)	6.32 (dd, 1H, H_X)	4.02 (d, 2H, CH_2)	
5	7.0–7.7 (m, 15H, Ar)	3.09 (dd, 1H, H_A, J_{AB}: 18.5, J_{AX}: 9.25)	3.6–3.5 (dd, 1H, H_B, J_{AB}: 16.6, J_{AX}: 9.52)	6.0–5.9 (dd, 1H, H_X, J_{AX}: 2.58, J_{BX}: 7.75)	3.51 (s, 3H, CH_3), 4.6 (d, 2H, CH_2)	7.7 (d, 1H, NH)
5a	7.23–7.76 (m, 15H, Ar)	3.31 (dd, 1H, H_A),	3.83 (dd, 1H, H_B)	5.91 (dd, 1H, H_X),	3.51 (s, 3H, CH_3), 4.66–3.22 (d, 2H, CH_2)	
6	6.77–7.20 (m, 15H, Ar)	3.31 (dd, 1H, H_A, J_{AB}: 17.2, J_{AX}: 10.5)	3.51 (dd, 1H, H_B, J_{AB}: 17.2, J_{BX}: 8.5)	5.3 (dd, 1H, H_X, J_{AX}: 10.5, J_{BX}: 8.5)	3.15–3.46 (m, 8H, CH_2)	8.01 (d, 1H, NH)
6a	7.50 (14H, m, Ar)	3.22 (dd, 1H, H_A, J_{AB}: 18.5, J_{AX}: 9.25)	3.49 (dd, 1H, H_B, J_{AB}: 18.5, J_{BX}: 9.25)	6.32 (dd, 1H, H_X, J_{AX}: 11.10, J_{BX}: 9.25)	3.03–3.10 (m, 8H, CH_2)	
7	6.67–7.75 (m, 15H, Ar)	3.31 (dd, 1H, H_A, J_{AB}: 17.33, J_{AX}: 9.33)	3.32 (dd, 1H, H_B, J_{AB}: 16.6, J_{AX}: 9.52)	6.09 (dd, 1H, H_X, J_{AX}: 10.5, J_{BX}: 8.5)	2.68 (s, 3H, CH_3), 2.11–2.32 (m, 8H, CH_2)	10.4 (s, 1H, NH)
7a	7.23–7.76 (m, 15H, Ar)	3.31 (dd, 1H, H_A)	3.83 (dd, 1H, H_B)	5.91 (dd, 1H, H_X)	3.51 (s, 3H, CH_3), 4.66–3.12 (m, 8H, CH_2)	
8	7.22–7.99 (m, 14H, Ar)	3.12 (dd, 1H, H_A, J_{AB}: 18.75, J_{AX}: 12.5)	3.41 (dd, H_B, CH_2, J_{AB}: 17.2, J_{BX}: 8.5)	6.09 (dd, H, H_X J_{AX}: 10.5, J_{BX}: 8.5)	1.68–2.39 (6H, m, CH_2)	7.7 (d, 1H, NH)
8a	7.23–7.76 (m, 15H, Ar)	3.31 (dd, 1H, H_A),	3.65 (dd, 1H, H_B)	5.16 (dd, 1H, H_X)	3.01–2.23 (m, 6H, CH_2)	

Table 5
^{13}C NMR spectroscopic data

Compound	[**1**–**8**, $CDC1_3$] and [**1a**–**8a**, $((CD_3)_2SO)$] (δ, ppm)
1	204.23 (C=S), 146.57 (C=N), 144.52–125.72 (phenyl-C), 17.90 (CH_3), 37.43 (CH_2), 62.86 (CH)
1a	198.23 (C=S), 146.57 (C=N), 144.52–125.72 (phenyl-C), 17.90 (CH_3), 37.43 (CH_2), 62.86 (CH)
2	175.49 (C=S), 143.85 (C=N), 148.52–115 (phenyl-C), 20.69 (CH_3), 37.43 (CH_2), 62.86 (CH)
2a	163.64 (C=S), 146.57 (C=N), 144.52–125.72 (phenyl-C), 17.90 (CH_3), 37.43 (CH_2), 62.86 (CH)
3	175.49 (C=S), 143.85 (C=N), 136.52–125 (phenyl-C), 21.00 (CH_3), 37.43 (CH_2), 62.86 (CH)
3a	163.64 (C=S), 146.57 (C=N), 144.52–125.72 (phenyl-C), 17.90 (CH_3), 37.43 (CH_2), 62.86 (CH)
4	177.42 (C=S), 150.29 (C=N), 150.02–129 (phenyl-C), 53.11 (CH_2), 37.09 (CH_2), 65.26 (CH)
4a	185.3 (C=S), 166.57 (C=N), 187.32–124.45 (phenyl-C), 97.19, 37.43 (CH_2), 60.96 (CH)
5	175.49 (C=S), 143.85 (C=N), 148.52–115 (phenyl-C), 24.08 (CH_3), 53.41, 37.43 (CH_2), 62.86 (CH)
5a	172.49 (C=S), 133.85 (C=N), 148.52–115 (phenyl-C), 24.08 (CH_3), 53.41, 37.43 (CH_2), 62.86 (CH)
6	187.49 (C=S), 150 (C=N), 154–117 (phenyl-C), 36.43, 53.80, 47.60 (CH_2), 66.28 (CH)
6a	204.23 (C=S), 146.57 (C=N), 144.52–125.72 (phenyl-C), 53.92, 41.04, 37.43 (CH_2), 62.86 (CH)
7	175.49 (C=S), 143.85 (C=N), 148.52–115 (phenyl-C), 51.04, 47.32, 38.17, 37.43 (CH_2), 62.86 (CH)
7a	172.14 (C=S), 149.25 (C=N), 144.52–128.72 (phenyl-C), 53.92, 41.04, 38.07, 37.43 (CH_2), 62.86 (CH)
8	186.94 (C=S), 154.25 (C=N), 150.52–118 (phenyl-C), 36.23, 37.18, 52.25, 38.63 (CH_2), 65.32 (CH)
8a	154.23 (C=S), 147.57 (C=N), 134.52–130.12 (phenyl-C), 53.92, 41.04, 39.89, 37.43 (CH_2), 63.89 (CH)

to produce a tri-substituted pyrazoline ion at *m/z* 330. Further elimination of 2-chlorobenzene radical gives rise to the formation of disubstituted pyrazoline ion at *m/z* 219, which was observed as a base peak. The removal of phenyl radical produced phenyl pyrazoline ion at *m/z* 142. At *m/z* 100, phenyl cyanide ion was also detected after the removal of azirinium radical from phenyl pyrazoline ion.

The mass spectra of metal complex **4a** also shows molecular ion peak (M + 1) at *m/z* 580, confirming their molecular weights and their fragmentation pathways can be initiated by the loss of two chlorine ions giving (M − Cl_2) at *m/z* 511.

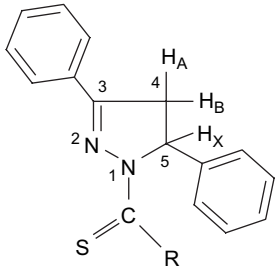

Fig. 1.

Table 6
ESI-MS

Compound	ESI-MS (*m/z*)
1	370 (M + 1), 221, 145, 104
1a	548, (M + 1), 515, 480
2	370 (M + 1), 221, 145, 104
2a	550 (M + 2), 514, 478, 370
3	369 (M + 2), 337, 311, 297, 221, 145, 104
3a	549 (M + 2), 515, 477, 372
4	404 (M + 1), 370, 330, 219, 142, 100
4a	580 (M + 2), 511, 405
5	383 (M + 2), 383, 354, 265, 223, 147, 105, 77
5a	560 (M + 2), 488, 380
6	425 (M + 1)
6a	605 (M + 2)
7	436 (M + 1)
7a	615 (M + 1)
8	398 (M + 1)
8a	575 (M + 1)

Elimination of Pd metal from thiocarbamoyl pyrazoline was observed at *m/z* 405 and further fragmentation followed the similar pathway as ligand.

2.4. Thermogravimetric analysis

The TGA (under nitrogen, rate 10%/min.) profiles of complexes along with the percentage weight at different temperatures were recorded (Table 7). The complexes do not lose weight up to 209 °C. Further increment of temperature causes the decomposition of the complexes in two steps. The temperature range for the first step begins at 209–270 °C where loss of chlorine and sulfur atoms from the complexes **3a**, **4a** and **5a** were observed. On the other hand complexes **1a**, **2a** and **6a**–**8a** showed the loss of mixed fragments. The second step starts immediately after first step and continues until complete decomposition of the ligand and formation of the end product as palladium sulfide (PdS).

2.5. In vitro antiamoebic activity

The in vitro activity of all the 1-*N*-thiocarbamoyl-3,5-diphenyl-2-pyrazolines and their Pd(II) complexes were compared with standard antiamoebic drug, metronidazole using *HM1:1MSS* strain of *E. histolytica* (Table 1). Metronidazole had a 50% inhibitory concentration ($IC_{50} = 1.82$ μM) in our experiment. The free ligands (**1**–**8**) showed IC_{50} value from 0.38 to 11.02 μM. The compounds **1**, **2** and **3** having methyl group at *ortho*, *meta* and *para* positions, respectively, showed that the compound **3** with methyl group at *para* position was found more active ($IC_{50} = 0.38$ μM) among the other two compounds. Incorporating palladium into the molecular structure of compound **3** enhances the activity ($IC_{50} = 0.05$ μM). The IC_{50} value for the Pd complex precursor was also determined, establishing that the metal complex precursor has no activity against *E. histolytica*. The distinct difference in the amoebicidal property of the

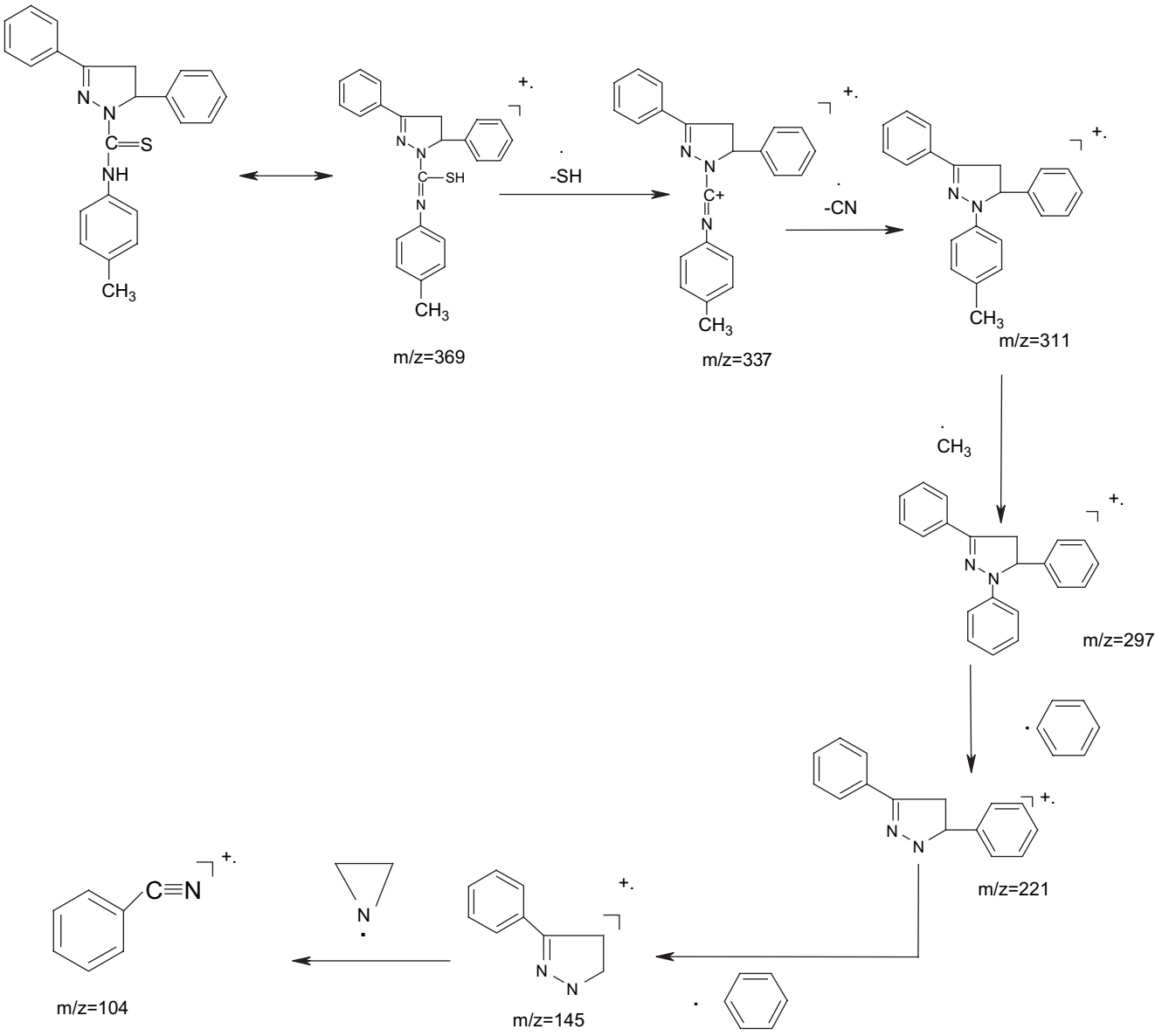

Scheme 2. Mass fragmentation pattern of compound **3**.

1-*N*-thiocarbamoyl-3,5diphenyl-2-pyrazoline derivatives and their metal complexes, **2a**–**8a** further justifies the purpose of this study. The importance of such work lies in the possibility that the new complexes might be more efficacious drugs against amoebiasis for which a thorough investigation regarding the structure–activity relationship, toxicity and in vivo studies of the complexes are in progress in order to understand the variation in their biological effects, which could be helpful in designing more potent antiamoebic agents for therapeutic use.

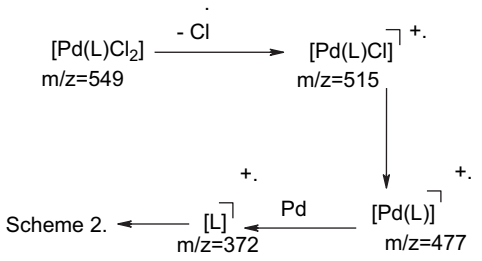

Scheme 3. Fragmentation pattern of compound **3a**.

3. Conclusion

This research involved the syntheses of new pyrazoline derivatives (**1**–**8**) and their palladium(II) complexes (**1a**–**8a**). On the basis of various studies square planar geometry for the complexes has been proposed. We have further examined the antiamoebic activities of all these new pyrazoline derivatives and their palladium(II) complexes. The biological behavior revealed that the complexes showed better activities than their corresponding ligands.

Table 7
Thermogravimetric analysis of compounds **1a–8a**

Compound	Thermogravimetric analyses
1a	Stability at ambient temp. 209 °C, first stage decomposition at 220 °C (Obs − 32.11, Calc − 32.29%), residue at 610 °C (Obs − 25.49, Calc − 25.18%).
2a	Stability at ambient temp. 210 °C, first stage decomposition at 230 °C (Obs − 32.5, Calc − 32.29%), residue at 620 °C (Obs − 25.1, Calc − 25.18%).
3a	Stability at ambient temp. 230 °C, first stage decomposition at 290 °C (Obs − 33.2, Calc − 32.29%), residue at 625 °C (Obs − 25.2, Calc − 25.18%).
4a	Stability to ambient temp. 209 °C, first stage decomposition at 280 °C (Obs − 30.05, Calc − 30.4%), residue at 585 °C (Obs − 24.32, Calc − 23.71%).
5a	Stability to ambient temp. 212 °C, first stage decomposition at 285 °C (Obs − 32.2, Calc − 31.49%), residue at 545 °C (Obs − 25.37, Calc − 24.55%).
6a	Stability at ambient temp. 210 °C, first stage decomposition at 300 °C (Obs − 30.01, Calc − 29.35%), residue at 615 °C (Obs − 23.1, Calc − 22.88%).
7a	Stability at ambient temp. 230 °C, first stage decomposition at 296 °C (Obs − 26.26, Calc − 28.78%), residue at 636 °C (Obs − 23.4, Calc − 22.4%).
8a	Stability at ambient temp. 230 °C, first stage decomposition at 290 °C (Obs − 31.45, Calc − 30.83%), residue at 625 °C (Obs − 25.2, Calc − 24.04%).

4. Experimental

4.1. Materials and methods

All the chemicals were purchased from Aldrich Chemical Company (U.S.A) and were used without further purification. The reactions were monitored by pre-coated aluminium silica gel 60 F_{254} thin layer plates procured from Merck (Germany). All thiosemicarbazides were prepared by a reported method [20] and their purity was confirmed by C, H and N analysis carried out at Central Drug Research Institute Lucknow, India. Chlorine was estimated by decomposing the complexes with Na_2O_2/NaOH and precipitated as AgCl with $AgNO_3$ after dissolving in dil. HNO_3. Melting points were recorded on KSW melting point apparatus and are uncorrected. Electronic spectra were recorded in methanol on a Shimadzu UV−1601PC UV−vis spectrophotometer. IR spectra on KBr disks were recorded on a Perkin−Elmer model 1620 FT-IR spectrophotometer. ^1H and ^{13}C NMR spectra were obtained at ambient temperature using a Brucker spectroscopin DPX-300 MHZ spectrophotometer in $CDCl_3$ using tetramethylsilane as an internal standard. The ESI mass spectra of a few representative compounds were recorded on a MICROMASS QUATTRO II triple quadrupole mass spectrometer.

4.2. Synthesis of thiocarbamoyl pyrazoline derivatives

Pyrazoline derivatives of chalcone have been prepared by the method reported in our previous paper [14]. A mixture of chalcone (10 mmol), thiosemicarbazide (10 mmol) and NaOH (25 mmol) was refluxed in ethanol (25 ml) for 8 h. The solution was poured in ice water. The precipitate was filtered and recrystallized from methanol.

4.3. General method for the synthesis of Pd(II) complexes

All Pd(II) complexes were prepared by a general procedure. In a typical procedure, $[Pd(DMSO)_2Cl_2]$ (1 mmol) was dissolved in 5 ml of methanol. Specific ligand (1 mmol) was added to the above and the reaction mixture was refluxed for 4 h. After cooling the solution was kept at 0 °C overnight, the solid mass separated out. It was filtered, washed with methanol and dried in vacuo.

4.4. In vitro testing against E. histolytica

All the cyclized pyrazoline analogues were screened in vitro for antiamoebic activity against (*HM1*:*1MSS*) strain of *E. histolytica* by microdilution method [21]. *E. histolytica* trophozoites were cultured in TYIS-33 growth medium as described previously in wells of 96-well microtiter plate [22]. All the compounds were dissolved in DMSO (40 μl) at which level no inhibition of amoeba occurs [23,24] and the stock solutions of the compounds were prepared freshly before use at a concentration of 1 mg/ml. Two-fold serial dilutions were made in the wells of 96-well microtiter plate (Costar). Each test includes metronidazole as a standard amoebicidal drug, control wells (culture medium plus amoebae) and a blank (culture medium only). The number of amoeba per milliliter was estimated with a heamocytometer and trypan blue exclusion was used to confirm viability. The cell suspension used was diluted to 10^5 organism/ml by adding fresh medium and 170 μl of this suspension was added to the test and control wells in the plate.

An inoculum of 1.7×10^4 organisms/well was chosen so that it is confluent, but not excessive growth took place in control wells. Plates were sealed and gassed for 10 min with nitrogen before incubation at 37 °C for 72 h.

4.5. Assessment of antiamoebic activity

After incubation, the growth of amoebae in the plate was checked with a low power microscope. Inverting the plate and shaking gently removed the culture medium. Plate was then immediately washed once in sodium chloride solution (0.9%) at 37 °C. This procedure was completed quickly, and the plate was not allowed to cool in order to prevent the

detachment of amoebae. The plate was allowed to dry at room temperature and the amoebae were fixed with methanol, and when dry, stained with (0.5%) aqueous eosin for 15 min. Stained plate was washed once with tape water and then twice with distilled water and allowed to dry. A 200 μl portion of 0.1 N sodium hydroxide solution was added to each well to dissolve the protein and release the dye. The optical density of the resulting solution in each well was determined at 490 nm with a microplate reader. The percentage inhibition of amoebal growth was calculated from the optical densities of the control and test wells and plotted against the logarithm of the dose of the drug tested. Linear regression analysis was used to determine the best-fitting straight line from which the IC_{50} value was found. The results are reported in Table 1.

Acknowledgements

This work was supported by Department of Science and Technology (Grant no. Vll-PRDSF/44/2004-05/TT). The authors are thankful to Prof. Alok Bhattacharya and Prof. Sudha Bhattacharya, School of Life Sciences and School of Environmental Sciences, Jawaharlal Nehru University, New Delhi, respectively, for providing laboratory facilities.

References

[1] M. Espinosa-Cantellano, A. Martinez-Palomo, Curr. Opin. Infect. Dis. 13 (2000) 451–456.
[2] F. Calzada, J.A. Cervantes-Martinez, L. Yepez-Mulia, J. Ethnopharmacol. 98 (2005) 191–193.
[3] F.D. Rocco, G. Sabatino, G. Tamburrini, O. Ranno, P. Valentini, M. Caldarelli, Acta. Neurochir. (Wein) 146 (2004) 1271–1272.
[4] M.E. Oxberry, R.C. Thompson, J.A. Reynoldson, Int. J. Parasitol. 24 (1994) 695–703.
[5] K. Kapoor, M. Chandra, D. Nag, J.K. Paliwal, R.C. Gupta, R.C. Saxena, Int. J. Clin. Pharmacol. Res. 19 (1999) 83–88.
[6] I.S. Adagu, D. Nolder, D.C. Warhurst, J.F. Rossignol, J. Antimicrob. Chemother. 49 (2002) 103–111.
[7] G.T. Zitouni, A. Ozdemir, K. Guven, Arch. Pharm. (Weinheim) 338 (2005) 96–104.
[8] O.A. Fathalla, M.E. Zaki, S.A. Swelam, S.M. Nofal, W.I. El-Eraky, Acta pol. Pharm. 60 (2003) 51–60.
[9] R. Mukherjee, Coord. Chem. Rev. 203 (2000) 151–218.
[10] S. Trofimenko, Prog. Inorg. Chem. 34 (1986) 115–210.
[11] A.P. Sadimenko, S.S. Basson, Coord. Chem. Rev. (1996) 147–247.
[12] G.L. Monica, G.A. Ardizzoia, Prog. Inorg. Chem. 46 (1997) 151–238.
[13] A.P. Sadimenko, Adv. Heterocycl. Chem. 80 (2001) 157–240.
[14] A. Budakoti, M. Abid, A. Azam, Eur. J. Med. Chem. 41 (2006) 63–70.
[15] M. Reyes-Lopez, S. Villa-Trevino, M. Arriaga-Alba, L. Aleman-Lazarini, M. Rodriguez-Mendiola, C. Arias-Castero, S. Fattel-Fazenda, G.D. la, Toxicol. In Vitro 19 (2005) 91–97.
[16] M.O. Albers, T.V. Ashworth, H.E. Oosthuizen, E. Singleton, Inorg. Synth. 26 (1989) 68–71.
[17] S. Sharma, F. Athar, M.R. Maurya, A. Azam, Eur. J. Med. Chem. 40 (2005) 1414–1449.
[18] N. Bharti, M.R. Maurya, F. Naqvi, A. Bhattacharya, S. Bhattacharya, A. Azam, Eur. J. Med. Chem. 35 (2000) 481–486.
[19] N. Gokhan, A. Yesilada, G. Ucar, K. Erol, A.A. Bilgin, Arch. Pharm. 336 (2003) 362–371.
[20] D.G. O'Sullivan, P.W. Sadler, C. Webley, Chemotherapy 7 (1963) 17–24.
[21] C.W. Wright, M.J. O'Neill, J.D. Phillipson, D.C. Warhurst, Antimicrob. Agents Chemother. 32 (1988) 1725–1729.
[22] L.S. Diamond, D.R. Harlow, C.C. Cunnick, Trans. R. Soc. Trop. Med. Hyg. 72 (1978) 431–432.
[23] F.D. Gillin, D.S. Reiner, M. Suffness, Antimicrob. Agents Chemother. 22 (1982) 342–345.
[24] A.T. Keen, A. Harris, J.D. Phillipson, D.C. Warhurst, Planta Med. (1986) 278–284.